Cargo-specific role for retriever subunit VPS26C in hepatocyte lipoprotein receptor recycling to control postprandial triglyceride-rich lipoproteins

Vos, D.Y.; Wijers, M.; Smit, M.; Huijkman, N.; Kloosterhuis, N.J.; Wolters, J.C.; ... ; Sluis, B. van de

Arteriosclerosis, Thrombosis, and Vascular Biology

BASIC SCIENCES

Cargo-Specific Role for Retriever Subunit VPS26C in Hepatocyte Lipoprotein Receptor Recycling to Control Postprandial Triglyceride-Rich Lipoproteins

Dyonne Y. Vos, Melinde Wijers, Marieke Smit, Nicolette Huijkman, Niels J. Kloosterhuis, Justina C. Wolters, Joël J. Tissink, Amanda C.M. Pronk, Sander Kooijman, Patrick C.N. Rensen, Jan Albert Kuivenhoven, Bart van de Sluis

BACKGROUND: The copper metabolism MURR1 domains/coiled-coil domain containing 22/coiled-coil domain containing 93 (CCC) complex is required for the transport of low-density lipoprotein receptor (LDLR) and LRP1 (LDLR-related protein 1) from endosomes to the cell surface of hepatocytes. Impaired functioning of hepatocytic CCC causes hypercholesterolemia in mice, dogs, and humans. Retriever, a protein complex consisting of subunits VPS26C, VPS35L, and VPS29, is associated with CCC, but its role in endosomal lipoprotein receptor transport is unclear. We here investigated the contribution of retriever to hepatocytic lipoprotein receptor recycling and plasma lipids regulation.

METHODS: Using somatic CRISPR/Cas9 gene editing, we generated liver-specific VPS35L or VPS26C-deficient mice. We determined total and surface levels of LDLR and LRP1 and plasma lipids. In addition, we studied the protein levels and composition of CCC and retriever.

RESULTS: Hepatocyte VPS35L deficiency reduced VPS26C levels but had minimal impact on CCC composition. VPS35L deletion decreased hepatocytic surface expression of LDLR and LRP1, accompanied by a 21% increase in plasma cholesterol levels. Hepatic VPS26C ablation affected neither levels of VPS35L and CCC subunits, nor plasma lipid concentrations. However, VPS26C deficiency increased hepatic LDLR protein levels by 2-fold, probably compensating for reduced LRP1 functioning, as we showed in VPS26C-deficient hepatoma cells. Upon PCSK9 (proprotein convertase subtilisin/kexin type 9)-mediated LDLR elimination, VPS26C ablation delayed postprandial triglyceride clearance and increased plasma triglyceride levels by 26%.

CONCLUSIONS: Our study suggests that VPS35L is shared between retriever and CCC to facilitate LDLR and LRP1 transport from endosomes to the cell surface. Conversely, retriever subunit VPS26C selectively transports LRP1, but not LDLR, and thereby may control hepatic uptake of postprandial triglyceride-rich lipoprotein remnants.

GRAPHIC ABSTRACT: A graphic abstract is available for this article.

Key Words: atherosclerosis ■ endosomes ■ gene editing ■ hepatocyte ■ liver

Atherosclerotic cardiovascular disease remains the leading cause of mortality worldwide.[1] It is well established that elevated plasma levels of LDL (low-density lipoprotein) cholesterol are causally related to atherosclerotic cardiovascular disease.[2] High plasma levels of TRLs (triglyceride-rich lipoproteins), and their remnants are nowadays also recognized as causal risk factors for atherosclerotic cardiovascular disease.[3,4] Hepatic uptake of these types of TRLs and remnants highly depends on the LDL receptor (LDLR) and LRP1 (LDLR-related protein 1), both members of the LDLR family.[5] LDLR mediates the clearance of LDL particles

Correspondence to: Bart van de Sluis, PhD, Department of Pediatrics, University Medical Center Groningen, UMC Groningen, Groningen 9713 AV, the Netherlands. Email a.j.a.van.de.sluis@umcg.nl
Supplemental Material is available at https://www.ahajournals.org/doi/suppl/10.1161/ATVBAHA.122.318169.
For Sources of Funding and Disclosures, see page e43.

Arterioscler Thromb Vasc Biol is available at www.ahajournals.org/journal/atvb

Nonstandard Abbreviations and Acronyms

apoB	apolipoprotein B
apoE	apolipoprotein E
CCDC22	coiled-coil domain containing 22
CCDC93	coiled-coil domain containing 93
COMMD	copper metabolism MURR1 domain
GST	glutathione S-transferase
ICD	intracellular domain
IDL	intermediate-density lipoprotein
LDL	low-density lipoprotein
LDLR	LDL receptor
LPL	lipoprotein lipase
LRP1	LDLR-related protein 1
PCSK9	proprotein convertase subtilisin/kexin type 9
TRL	triglyceride-rich lipoprotein
VLDL	very-low–density lipoprotein
VPS	vacuolar protein sorting
WASH	Wiskott-Aldrich syndrome protein and SCAR homolog

Highlights

- Endosomal recycling of lipoprotein receptors is tightly regulated to control hepatic lipoprotein uptake.
- VPS35L is shared by retriever and CCC complex and is required for plasma cholesterol homeostasis by facilitating the transport of LDLR (low-density lipoprotein receptor) and LRP1 (LDLR-related protein 1) to the plasma membrane of hepatocytes.
- Retriever subunit VPS26C selectively controls the recycling of LRP1, but not low-density lipoprotein receptor, and regulates clearance of postprandial remnant lipoproteins.

through binding to apoB (apolipoprotein B), and of TRL remnants, such as chylomicron remnants and VLDL (very-low–density lipoprotein) remnants through binding of apoE (apolipoprotein E).[6,7] Although the contribution of hepatic LRP1 to plasma lipid clearance is less clear, several studies have demonstrated a role in the hepatic uptake of chylomicron remnants.[8–11] In addition, genetic studies have identified a single nucleotide polymorphism in the *LRP1* locus associated with triglyceride (TG) levels.[12,13]

LDLR and LRP1 are both regulated at transcriptional and posttranslational levels,[14–19] but in recent years, it has become clear that the endosomal sorting system also plays a crucial role in their functioning and, consequently, in the hepatic uptake of lipoproteins (reviewed by Wijers et al,[20] Van De Sluis et al,[21] and Vos et al[22]). After endocytosis, these receptors are transported from the endosome back to the cell surface for reuse, or alternatively, directed to lysosomes for degradation.[23] These sorting pathways are tightly regulated by various protein complexes, and multiple studies have illustrated that mutations in these protein complexes result in dyslipidemia in mice, dogs, and humans.[24–26] Hepatic loss of the endosomal sorting complexes copper metabolism MURR1 domain (COMMD)-coiled-coil domain containing 22 (CCDC22)-coiled-coil domain containing 93 (CCDC93; CCC) or Wiskott-Aldrich syndrome protein and SCAR homolog (WASH) impairs the transport of LDLR and LRP1 from endosomes to the cell surface, resulting in elevated plasma LDL cholesterol and impaired clearance of chylomicron remnants.[24–26] Furthermore, a common genetic variant in CCC subunit *CCDC93* is associated with reduced LDL cholesterol levels, and lower risk of myocardial infarction and cardiovascular mortality. This was explained by enhanced functioning of the CCC complex, resulting in improved LDLR recycling.[27]

In vitro studies have shown that the localization of the WASH and CCC complexes to endosomes partially depends on the trimeric protein complex retromer (vacuolar protein sorting [VPS] 35, VPS26, VPS29), a key regulator of endosomal cargo sorting.[28–30] Interestingly, a recent study identified a novel protein complex called retriever, which is composed of VPS26C, VPS35L, and VPS29 (Figure 1A). Retriever physically associates with CCC and WASH complexes at endosomes to form a retromer-independent endosomal sorting pathway.[31] It shows structural similarities with retromer and they both contain a VPS29 subunit.[31] Retriever likely facilitates receptor recycling through coupling of VPS26C to the adaptor protein sorting nexin (SNX) 17, whereas retromer recognizes receptors via the adaptor protein SNX27.[31] Previous in vitro studies have demonstrated that SNX17 mediates endosomal sorting of cargos containing a NPxY/NxxY-motif in their cytoplasmic domain, including LDLR and LRP1.[5,32–36] However, to date, there is no evidence whether retriever is required for the endosomal transport of hepatocytic LDLR and LRP1. Moreover, the authors who described retriever also suggested that the protein VPS35L, previously known as C16orf62 and originally identified as a subunit of the CCC complex,[28] participates in retriever and not in CCC.[31] In contrast, a recent study showed that VPS35L is a shared subunit between retriever and CCC.[37] We showed a strong reduction in VPS35L protein levels upon hepatic depletion of one of the CCC subunits—either CCDC22 or one of the ten members of the COMMD family of proteins[25,38]—suggesting that VPS35L participates in CCC complex formation, and does not form a distinct protein complex. In line with this, systems biology studies have suggested that CCC and retriever likely form a large evolutionary conserved multiprotein complex, named COMMander.[39]

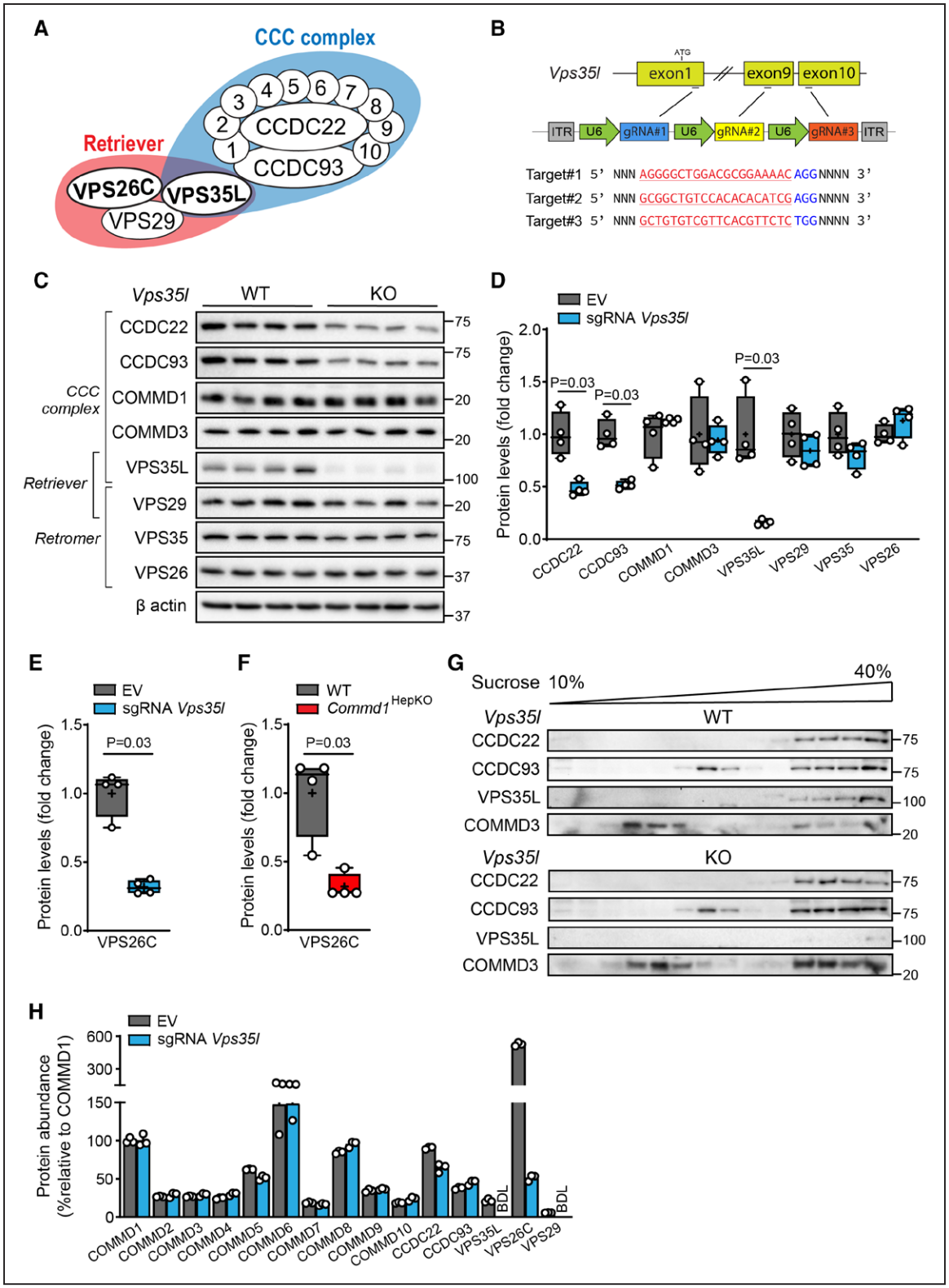

Figure 1. Loss of hepatic VPS35L slightly affects the integrity of the CCC complex.
A, Overview of retriever and CCC complex and their subunits. Subunits shown as 1 to 10 indicate the COMMD proteins. In the current study, we have specifically investigated the role of subunits VPS26C and VPS35L, indicated in bold. **B**, Schematic illustration of single-vector AAV (adeno-associated virus) system used for targeting *Vps35l* in hepatic Cas9-expressing mice. Target sequences are shown in red and PAM sequences in blue. **C**, Hepatic protein levels of CCC complex, retriever and retromer subunits determined by immunoblotting (n=4). **D**, Quantification of immunoblot results (n=4) shown in **C**. Data are presented as median with min-to-max whiskers (mean indicated by +); groups were compared using Mann-Whitney *U* test. **E**, VPS26C protein levels in control and VPS35L-deficient livers, (*Continued*)

Taken together, these contradictory findings show that neither the molecular organization nor the physiological role of retriever in endosomal sorting are as yet fully understood. In the current study, we systematically investigated the role of retriever in hepatocyte lipoprotein receptor-mediated lipoprotein uptake in mice. We show that hepatic VPS35L mediates the endosomal transport of LDLR and LRP1 to the cell surface, thereby regulating plasma LDL cholesterol levels in mice. Conversely, retriever subunit VPS26C has a specific role in transport of lipoprotein receptors, as it regulates LRP1 functioning, but not LDLR, to facilitate hepatic uptake of postprandial TRL remnants.

MATERIALS AND METHODS

The data that support the findings of this study are available to other researchers upon reasonable request to the corresponding author.

Animals

To generate mice with hepatocyte-specific Cas9 expression, Rosa26-LSL-Cas9 knock-in mice (#026175, The Jackson Laboratory)[40] were crossed with Albumin-Cre mice (#003574, The Jackson Laboratory). *Vps35l* and *Vps26c* were targeted in mouse hepatocytes, using CRISPR/Cas9 gene editing technology.[25] To blunt hepatic LDLR expression, mice were injected with 3×10^{11} vector genomes of AAV (adeno-associated virus)-PCSK9 (proprotein convertase subtilisin/kexin type 9)-D377Y by means of retro-orbital injection, as previously described.[25] Liver-specific *Commd1* knockout mice were previously described.[24,41]

All animal procedures were approved by the Institutional Animal Care and Use Committee, University of Groningen (Groningen, the Netherlands). Male mice (C57BL/6J background, littermates, 8–12 weeks of age at the time of gene editing) were used for all experiments and were individually housed under a 12-hour light-dark cycle (lights on at 8:00) with ad libitum access to standard laboratory diet (10% fat, 23% protein, and 67% carbohydrates; V1554-703, Ssniff Spezialdiäten GmbH) and water. Prior to sacrifice, mice were fasted for 4 hours. Upon sacrifice, liver tissue was collected and snap-frozen in liquid nitrogen and stored at −80 °C until further analysis. Blood was collected by cardiac puncture into EDTA-coated tubes, and plasma was collected after centrifugation at 1000×*g* for 10 minutes at 4 °C. Only male mice were used to compare our results with previous studies in which we investigated the role of the endosomal sorting machinery in cholesterol homeostasis[24–26]; using only male mice is a limitation of the current study. Sample size of each experiment is described in the figure legends, no randomization or blinding methods were used for the animal studies.

Oral Fat Tolerance Test

Mice were fasted for 5 hours (from 8:00 to 13:00) prior to receiving an oral gavage of olive oil (Bertolli; 4 µl per g body weight). Blood samples were collected from the tail vein at 30, 60, 90, 120, 180, and 240 minutes after gavage into EDTA-coated tubes. After centrifugation at 1000×*g* for 10 minutes at 4 °C, plasma was collected and used for TG measurements.

Plasma Clearance and Tissue Uptake of VLDL-Mimicking Particles

After a 4-hour fast (from 9:00 to 13:00), mice were injected intraperitoneally with glucose (2 g per kg body weight). Thirty minutes after glucose injection, conscious mice were injected via the tail vein with VLDL-mimicking particles (80 nm) labeled with glycerol tri[^{3}H]oleate (TO) and [^{14}C]cholesteryl oleate (CO), prepared as previously described.[42] Blood sampling from the tail vein was done at 2, 5, 10, and 15 minutes to determine the plasma decay of [^{3}H]TO and [^{14}C]CO. After 15 minutes, animals were sacrificed and perfused with ice-cold PBS. Tissues were collected to determine the tissue-specific uptake of [^{3}H]TO and [^{14}C]CO-derived activity.

VLDL-TG Production Assay

Following a 4-hour morning fast (from 8:00 to 12:00), mice were intraperitoneally injected with Poloxamer 407 (Sigma) solution in PBS (1 g per kg body weight) to block lipoprotein lipase activity. Blood samples were collected in EDTA-coated tubes from the tail vein at time points 0, 30, 60, 120, and 240 minutes after Poloxamer 407 injection. Plasma was collected after centrifugation at 1000×*g* for 10 minutes at 4 °C, and was used for TG measurements.

Hepatic Lipid Extraction

Lipid extraction was performed on liver homogenates (15% w/v in PBS) following the Bligh and Dyer method.[43] In brief, 200 µl of liver homogenate was added to 600 µl of demi-water and subsequently mixed with 3 ml chloroform/methanol (1:2 v/v) in a glass tube. After 30 minutes of incubation, 1.2 ml of H_2O and 1 ml of chloroform were added, mixed, and centrifuged at 500×*g* for 10 minutes at room temperature. After transferring the organic layer to a new glass tube, solvent was evaporated with nitrogen at 50 °C. Dried lipids were dissolved in 1 ml chloroform and used for quantification of cholesterol and triglyceride content.

Cholesterol and Triglyceride Measurements in Plasma and Liver

Total cholesterol concentrations were quantified with colorimetric assays, using cholesterol enzymatic reagents (#11489232,

Figure 1 Continued. determined by targeted proteomics (n=4). **F**, VPS26C protein levels in livers of WT and hepatic COMMD1-deficient mice, determined by targeted proteomics (n=4). **G**, Immunoblot of control and VPS35L-deficient liver lysates after fractionation on a 10% to 40% sucrose gradient. **H**, Protein levels of CCC complex and retriever subunits relatively associated with COMMD1, assessed by immunoprecipitation of COMMD1 in control and VPS35L-deficient primary hepatocytes and determined by targeted proteomics (n=3, technical replicates; shown as mean±SEM). **D**–**F**, Data are presented as median with min-to-max whiskers (mean indicated by +); groups were compared using Mann-Whitney *U* test. **D**, *P* after parametric *t* test and correction for multiple testing: *P*=0.02 (CCDC22); *P*=0.004 (CCDC93); and *P*=0.02 (VPS35L). BDL indicates below detection level.

Roche; Cholesterol FS, DiaSys), with the cholesterol standard FS (DiaSys) as a reference. Triglyceride levels were determined using a Trig/GB kit (#1187771, Roche) or Triglycerides FS (DiaSys), with the Precimat Glycerol standard (Roche) as a reference.

Fast-Performance Liquid Chromatography

Total cholesterol and triglyceride content of the major lipoprotein classes (VLDL, LDL, and HDL) was assessed using FPLC analysis. In short, the system consisted of a PU-4180 RHPLC pump and a UV-4075 UV-Vis detector (Jasco). Measurements were performed in either individual plasma samples when enough sample available, or in pooled plasma samples. To minimize inaccuracies as a consequence of pooling samples for FPLC as described in the AHA statement,[44] no selection criteria were used to select specific samples, thus we have pooled equal volumes of all individual samples for each experimental group of mice (see figure legends for details on individual or pooled measurements). Samples were diluted in PBS, and loaded onto a Superose Increase 10/300 GL column (GE Healthcare) for separation of lipoproteins at a flow rate of 0.31 mL/min. A second flow was used to add cholesterol (Roche) or triglyceride enzymatic reagents (DiaSys) at a flow rate of 0.1 ml/min.

Sucrose Gradients

Two hundred milligrams of snap-frozen liver tissue were homogenized in 800 µl homogenization buffer (50 mM Tris-HCl [pH 7.4], 250 mM sucrose, 25 mM KCl, 5 mM $MgCl_2$, 3 mM imidazole, supplemented with protease inhibitors [Roche]). Homogenates were centrifuged at 1000x*g* for 10 minutes at 4 °C to remove nuclei and other debris. Protein concentrations were determined with the Bradford method (Bio-Rad) and 1.5 mg of liver homogenates were loaded into a 3.7 ml continuous 10% to 40% sucrose gradient. Samples were centrifuged using a Beckman Coulter SW55 Ti rotor for 16 hours at 40 000 rpm. Then, 360 µl fractions were collected from the top with the use of a pipet, and 1/5 of each fraction was mixed with 2× SDS sample buffer for further analysis by immunoblotting.

Generation of Adeno-Associated Virus

Gene blocks, consisting of 3 single guide RNAs (sgRNAs) targeting *Vps35l* or *Vps26c*, were ordered (ThermoFisher); the complete sequences are available upon request. A pscAAV-Basic vector was constructed with the backbone of the scAAV-LP1-hFIXco plasmid.[45] The original Lp1 promotor and FIX-coding sequences were replaced with stuffer DNA and a multiple cloning site containing KpnI and NotI restriction sites. The sgRNA expression cassette was ligated into the KpnI/NotI-linearized pscAAV vector. Using the polyethylenimine (PEI) method, this scAAV vector was transfected into HEK293T (ATCC #CRL-11268) cells, together with Adenoviral helper plasmid pAdDeltaF6 (Addgene #112867) and AAV8 packaging vector pAAV2/8 (Addgene #112864). scAAV particles were harvested 54 hours after transfection and purified overnight, using an iodixanol gradient, as previously described.[46] Purified virus was aliquoted and stored at −80 °C. scAAV particles were titrated by qPCR using 2 primer-probe sets targeting spacerDNA, F1: tgaccatcatgttttattgccat, R1: tccagaatttgatcctgcatg, P1:tccaaatctgtcagcatctgggtcattc a; F2: tcgcgttgttttcttcaccttt, R2: agttaaagcagctggtggagt, P2: ccaccacttgttcctaagcggtcagc. The number of genomic copies scAAV per ml was derived from the standard curve of known scAAV vector copies.

Cell Culture

VPS26C was ablated in Hepa1-6 murine hepatoma cells stably expressing Cas9. These cells were kindly donated by Noam Zelcer.[47] Cells were transduced (MOI=25) with adenovirus containing sgRNAs targeting *Vps26c* (Figure 3A). Adenovirus was generated as previously described.[25] After transduction, single colonies were selected and analyzed for VPS26C expression. Control cells were transduced with adenovirus without sgRNAs and were treated as the VPS26 knockout cells. The cells were cultured in Dulbecco's modified Eagle medium (DMEM) GlutaMAX (Gibco), supplemented with 10% fetal calf serum, 1% penicillin-streptomycin solution, and 1.25 µg/ml puromycin, at 37 °C and 5% CO_2.

Primary murine hepatocytes were prepared as described previously.[11] In brief, hepatocytes were isolated by liver perfusion and EDTA dissociation, and were then separated from non-parenchymal cells by centrifugation using a Percoll gradient. Hepatocytes were seeded in DMEM supplemented with 10% fetal calf serum and 1% antibiotics in collagen-coated plates, and subsequently used for immunoprecipitation experiments and biotinylation assays.

Human embryonic kidney 293T (HEK293T) cells (American Type Culture Collection) were cultured in DMEM GlutaMAX (Gibco) supplemented with 10% fetal calf serum and 1% penicillin-streptomycin solution and were used for pulldown experiments.

GST-Pulldown and Immunoprecipitation Experiments

GST (glutathione S-transferase) pulldown assays were performed in HEK293T cells as previously described.[24] In brief, cells were co-transfected with Flag-VPS26C construct and either GST alone, GST-LDLR intracellular domain (ICD; GST-tagged intracellular domain of LDLR),[25] or GST-LRP1 ICD. Construct containing GST-tagged ICD of LRP1 was kindly provided by Jörg Heeren[11] and insert was subcloned into pEBB-GST[24] using *BamHI* and *NotI* sites. Cells were lysed in NP-40 buffer (0.1% Nonidet P-40 [NP-40], 0.4 M NaCl, 10 mM Tris-HCl [pH 8.0], 1 mM EDTA) supplemented with protease inhibitors. Lysates were then incubated with Glutathione Sepharose 4B beads (GE Healthcare Life Sciences) at 4 °C for 2 hours to purify the GST-tagged proteins. Flag- and GST-tagged proteins were detected by immunoblotting.

Immunoprecipitation of COMMD1 was performed in primary hepatocytes as previously described.[25] Cells were lysed in NP-40 buffer supplemented with protease inhibitors, and cell lysates were incubated with anti-COMMD1 antibody for 1 hour at 4°C. Subsequently, protein A/G-agarose beads (Santa Cruz) were added and lysates were incubated for 2 hours at 4°C. Proteins interacting with COMMD1 were detected by targeted proteomics.

Biotinylation Assay

For biotinylation assays, cells were washed 3 times with ice-cold PBS-CM buffer (PBS with 1 mM $MgCl_2$, 0.5 mM $CaCl_2$) and subsequently incubated with 0.5 mg/ml EZ-Link

Sulfo-NHS-SS Biotin (Thermo Scientific) in PBS-CM for 30 minutes at 4 °C. After removing the biotinylation reagent, cells were washed twice with PBS-CM containing 0.1% BSA to quench unbound biotin, and once with PBS-CM. Cells were lysed in lysis buffer (50 mM Tris-HCl [pH 7.5], 150 mM NaCl, 1% NP-40, 5 mM EDTA, supplemented with protease inhibitors (Roche)) and after 5 minutes of incubation at 4 °C, cells were collected by scraping. Cells were centrifuged at 4 °C (14 000×*g*, 10 minutes); supernatants were transferred to a new tube and used to determine protein concentrations using the Bradford assay (Bio-Rad). Two milligrams of protein were diluted in lysis buffer and added to 80 µl Neutravidin beads (Neutravidin Agarose resin, Thermo Scientific). After 2 hours of incubation at 4 °C, beads were collected by centrifugation (500×*g*, 2 minutes at 4 °C), and washed twice with lysis buffer containing 1 mM biotin, and 3 times with lysis buffer alone. To elute the proteins, beads were resuspended in 50 µl 2× SDS sample buffer.

Gene Expression Analysis

Hundred milligrams liver samples were homogenized in 1 ml QIAzol Lysis Reagent (Qiagen). After isolation of total RNA by chloroform extraction, RNA was precipitated with isopropanol and washed with ethanol. RNA pellets were dissolved in RNase/DNase-free water, and 2 µg of RNA were used for synthesis of cDNA with the Transcriptor Universal cDNA Master kit (Roche), according to the manufacturer's instructions. Subsequently, 20 ng of cDNA were used for quantitative reverse transcription PCR, which was performed using the FastStart SYBR Green Master (Roche) and the QuantStudio 7 Flex Real-Time PCR System (Applied Biosystems). The qRT-PCR program was as follows: 50 °C/2 minutes; 95 °C/10 minutes; 40 cycles with 95 °C/15 sec; and 60 °C/1 minutes. Relative gene expression was calculated using the ΔΔCT method with QuantStudio Real-Time PCR Software (Applied Biosystems); *Ppia* expression was used as an internal control.

Immunoblotting

Cells and snap-frozen liver tissue samples were lysed in NP-40 buffer (0.1% Nonidet P-40 [NP-40], 0.4 M NaCl, 10 mM Tris-HCl [pH 8.0], 1 mM EDTA) supplemented with 1 mM DTT and protease and phosphatase inhibitors (Roche). Protein concentrations were determined using the Bradford assay (Bio-Rad). Proteins were separated with SDS-PAGE and subsequently transferred to Amersham Hybond-P PVDF Transfer Membrane (GE Healthcare; RPN303F). Membranes were blocked for 1 hour in 5% milk in Tris-buffered saline with 0.01% Tween 20, followed by incubation with the indicated antibodies (see Major Resources Table in the Supplemental Material for information about the antibodies). Proteins were visualized with the ChemiDoc XRS+ System, using Image Lab software version 5.2.1 (Bio-Rad).

Targeted Proteomics Analysis

To determine protein concentrations of the COMMDs and subunits of retromer, CCC, and WASH complexes in Hepa1-6 cells, liver lysates and IP samples, and apoA1 and apoB100 in plasma, we used targeted proteomic assays as previously described,[25] with a partly extended panel of screened target proteins, such as VPS26C. For proteomics analysis of plasma samples, 6 representative samples were selected from each group. In short, target peptides were concatenated into synthetic proteins (or "QconCATs"; Polyquant GmbH), with ^{13}C-labeled arginines and lysines. Concentrations of these isotopically labeled QconCATs served as standards to calculate the concentrations of endogenous equivalents of the peptides. In-gel digestion of the samples was performed as described previously,[25] with the following modifications: digestion was performed on 50 µg total protein of liver lysates, 37.5 µg total protein of Hepa1-6 cell lysates, 1 µl of plasma samples, and 35 µl of IP-enriched samples. One band containing all proteins was excised from the gel, except when quantifying COMMD proteins in liver lysates, for which a separate gel band specifically enriched with small proteins (including COMMD proteins) was excised. Isotopically labeled standard peptides were added prior to the liquid chromatography-mass spectrometry (LC-MS) detection. The amount of sample and QconCATs injected in the LC-MS were optimized for each experiment. The list of peptides for each target protein used in this study is shown in the Major Resources Table in the Supplemental Material.

Statistical Analysis

Statistical analyses were performed with GraphPad version 9.1 (GraphPad software). Data were checked for normality by Shapiro-Wilk test and for equal variance by the *F* test. For normally distributed data, differences between 2 groups were determined using unpaired Student *t* test, or Welch *t* test in case of unequal variances, and data are expressed as mean±SEM. For non-normally distributed data, or when sample size n≤5, Mann-Whitney *U* test was used, and data are expressed as median with min-to-max whiskers. To correct for multiple testing, the Holm-Šídák multiple comparison test was in several cases also performed, as indicated in the figure legends (Figures 1D and 3D; Figure S1A). Since a property of the non-parametric test is that P=0.0286 is the minimum P possible when n=4/group, multiple comparison testing was in some cases also performed after a parametric *t* test (Figure 1D; Figure S1A). These P are reported in the figure legends of Figure 1D and Figure S1A. For longitudinal measurements, repeated measures ANOVA with Geisser-Greenhouse correction and Šidák's multiple comparison test was performed. For all experiments, $P<0.05$ were considered statistically significant.

RESULTS

Retriever has recently been identified as a trimeric protein complex consisting of VPS26C, VPS29, and VPS35L (Figure 1A), which is physically associated with the CCC complex.[31] It has initially been suggested that VPS35L forms the CCC complex together with CCDC93, CCDC22 and 10 COMMD proteins[28] (Figure 1A), while others recognize VPS35L as a shared subunit between both complexes,[37] or that it participates in 1 large multiprotein complex called COMMander.[39] To date, there is no consensus whether VPS35L is a shared subunit between the 2 complexes or participates in only one of the 2 complexes. To elucidate the molecular organization of retriever and its physiological role in endosomal

sorting of lipoprotein receptors, we first generated and studied a mouse model with a hepatocyte-specific deletion of VPS35L, followed by a mouse model with a hepatocyte-specific deletion of retriever subunit VPS26C. The role of VPS29 was not investigated in the current study, since this subunit is a subunit of retriever and retromer, and loss of VPS29 would therefore negatively affect retriever as well retromer.[31]

Hepatic VPS35L Depletion Marginally Affects CCC Complex Integrity but Strongly Reduces VPS26C Levels

It has recently been reported that VPS35L is a subunit shared by the CCC complex and retriever[37] (Figure 1A). As previous studies have shown that the integrity of the CCC complex is dependent on all its core subunits,[25,28] we examined the effect of hepatocyte VPS35L depletion on the protein levels of CCC and retriever subunits. VPS35L was deleted specifically in mouse hepatocytes, using CRISPR/Cas9 somatic gene editing technology. Three sgRNAs were designed to target exons 1, 9, and 10 of *Vps35l* (Figure 1B) and were expressed in livers of hepatocyte-specific Cas9-expressing mice using AAV. Using this approach, the hepatic levels of VPS35L were decreased by 84%. This resulted in a 52% and 48% reduction of the protein levels of the CCC core components CCDC22 and CCDC93, respectively (Figure 1C and 1D). Hepatic ablation of VPS35L did not decrease the protein levels of COMMD1 and COMMD3 (Figure 1C and 1D), which was confirmed by targeted proteomics analysis (Figure S1A). Although VPS35L deficiency had only a very mild impact on the levels of most of the COMMD proteins, COMMD10 levels were decreased by 42% (Figure S1A). The protein levels of retromer subunits VPS35 and VPS26 were also not affected by the loss of VPS35L, nor was VPS29, a subunit of retromer and retriever[31] (Figure 1C and 1D). However, retriever component VPS26C was reduced by 68% upon VPS35L ablation (Figure 1E). The same level of reduction in VPS26C was observed in mice lacking CCC subunit COMMD1 in their livers (Figure 1F).

To further elucidate the impact of VPS35L depletion on the formation of the CCC complex, we assessed the cellular distribution of CCC subunits CCDC22, CCDC93, and COMMD3 by continuous sucrose gradient fractionation of mouse livers. Despite the reduced levels of CCDC22 and CCDC93 (Figure 1C and 1D), loss of hepatocytic VPS35L did not affect their distribution (Figure 1E). Next, we immunoprecipitated the CCC complex through COMMD1 in primary hepatocytes of control and hepatic VPS35L-deficient mice, and used targeted proteomics to analyze the protein levels of CCC and retriever subunits associated with COMMD1. We found that VPS35L deficiency reduced the levels of CCDC22 by 29% but did not affect the levels of other CCC subunits associated with COMMD1 (Figure 1H). However, loss of VPS35L reduced the binding between COMMD1 and retriever subunit VPS26C by 90% (Figure 1H) and blunted the interaction of retriever subunit VPS29 with the CCC complex (Figure 1H). Since total protein levels of VPS29 were not changed upon VPS35L ablation (Figure 1C and 1D), these data indicate that VPS35L is needed for the physical association between retriever and the CCC complex without having a strong adverse effect on CCC complex composition. Overall, these findings show that hepatic loss of VPS35L slightly affects CCC complex formation without having an impact on retromer, but strongly reduces the protein level of retriever component VPS26C and the association between of VPS29 and CCC, and thus seems to be required to connect the CCC complex and retriever with each other.

Hepatic Loss of VPS35L Results in Hypercholesterolemia in Mice

We have previously demonstrated that loss of the CCC complex in hepatocytes impairs endosomal recycling of LDLR and LRP1, resulting in hypercholesterolemia.[24,25] Although hepatic VPS35L deficiency minimally affects CCC complex integrity, we still assessed whether hepatic VPS35L is required to transport LDLR and LRP1 from the endosomes to the cell surface. Using a biotinylation assay, we determined the plasma membrane levels of LDLR and LRP1 in primary hepatocytes of control and hepatic VPS35L-deficient mice. In line with COMMD1- and COMMD6-deficient hepatocytes,[24,25] VPS35L ablation strongly reduced total LDLR and LRP1 levels, as well as levels at the plasma membrane (Figure 2A); this can probably be explained by impaired endosomal receptor recycling, resulting in increased lysosomal degradation.[24,25] In line with a loss of these receptors on the cell membrane, hepatic ablation of VPS35L resulted in a 21% increase in plasma cholesterol levels (Figure 2B). Separation of plasma by fast protein liquid chromatography (FPLC) revealed that the relative cholesterol content was increased mainly in LDL fractions (Figure 2C), which was supported by increased apoB100 levels in the plasma (Figure 2D). These data show that hepatic ablation of VPS35L impairs the endosomal transport of LDLR and LRP1 and mimics the hypercholesterolemic phenotype of hepatocyte-specific CCC-deficient mice,[24,25] which may suggest that VPS35L and CCC act together to control plasma cholesterol levels.

Ablation of Hepatic VPS26C Does Not Affect the Integrity of the CCC Complex

Next, we assessed the effect of retriever subunit VPS26C (Figure 1A) on CCC function and regulation of plasma lipid levels. As with VPS35L ablation, we applied

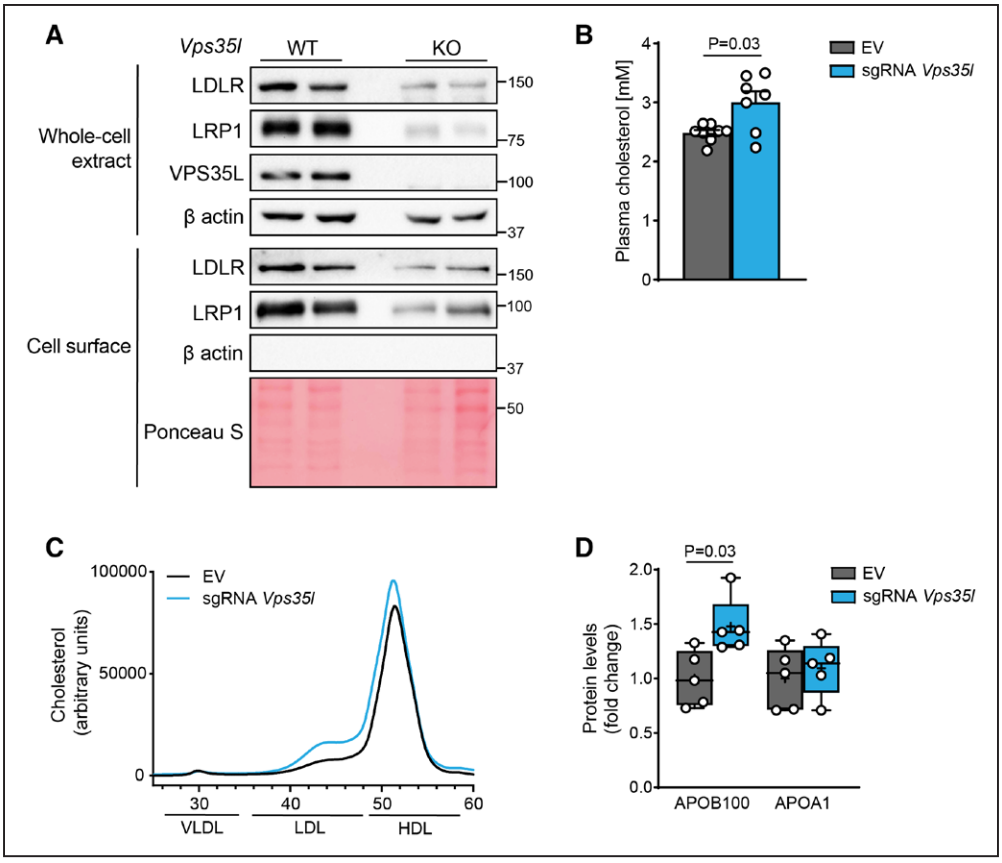

Figure 2. Hepatic VPS35L is required for the expression of low-density lipoprotein receptor (LDLR) and LRP1 (LDLR-related protein 1) at the plasma membrane and maintaining plasma cholesterol homeostasis.
A, Protein levels of LDLR and LRP1 in whole-cell extracts and at the cell surface of control and VPS35L-deficient primary hepatocytes determined by immunoblotting. **B**, Plasma cholesterol levels in control and hepatic VPS35L-deficient mice (n=7–8), 4 weeks after CRISPR/Cas9-mediated gene editing. **C**, Cholesterol levels in pooled plasma fractionated by FPLC of control and hepatic VPS35L-deficient mice (n=one pooled sample from 8 controls or 7 hepatic VPS35L-deficient mice). **D**, Plasma levels of apoB100 and apoA1 in control and hepatic VPS35L-deficient mice (n=5), 4 weeks after CRISPR/Cas9-mediated gene editing. Data are presented as mean±SEM (**B**) or median with min-to-max whiskers (mean indicated by +; **D**); groups were compared using Welch *t* test (**B**) and Mann-Whitney *U* test (**D**).

CRISPR/Cas9 somatic gene editing to deplete VPS26C specifically in the hepatocytes of mice. Hepatocyte-specific expression of 3 sgRNAs targeting exon 1 of *Vps26c* (Figure 3A) resulted in efficient editing of the *Vps26C* locus, as determined by RT-PCR analysis using primers annealing to the sequence edited by CRISPR/Cas9 (Figure 3B); this resulted in a 75% reduction of VPS26C protein levels (Figure 3B). Although the protein level of the CCC subunit CCDC22 tend to increase upon hepatocyte VPS26C deletion, the level of the other CCC subunits CCDC93, COMMD1, and VPS35L were unaffected, as assessed by Western blot analysis (Figure 3C and 3D). Retromer subunit VPS35 was significantly reduced by 39%, but the other retromer subunits, VPS26 and VPS29, were not affected by VPS26C deletion (Figure 3C and 3D). These data suggest that VPS26C deficiency neither adversely affects the integrity of the CCC complex and retromer, nor the protein levels of VPS35L. Thus, this model allows us to study the specific role of retriever in LDLR and LRP1 functioning and plasma lipids regulation.

Hepatic Loss of VPS26C Upregulates LDLR Protein Levels Without Affecting Plasma Lipid Levels

To evaluate the effect of VPS26C depletion on the function of LDLR and LRP1, we first determined the total LDLR and LRP1 protein levels in livers of hepatocyte specific VPS26C-deficient mice. While LRP1 protein levels were unchanged, we found that LDLR protein levels were almost doubled upon VPS26C ablation (Figure 4A and 4B), which could not be explained by changes in mRNA levels (Figure 4C). However, despite increased LDLR protein levels, plasma cholesterol and TG levels were not affected by *Vps26c* editing (Figure 4D through 4F).

Since *Ldlr* expression was not changed, the increased LDLR protein levels could be explained by a post-translational event. Similar observations were reported in studies that investigated the effect of dysfunctional LRP1—either by LRP1 deficiency or compromised LRP1 trafficking—on lipid homeostasis.[8,9,11,48] In

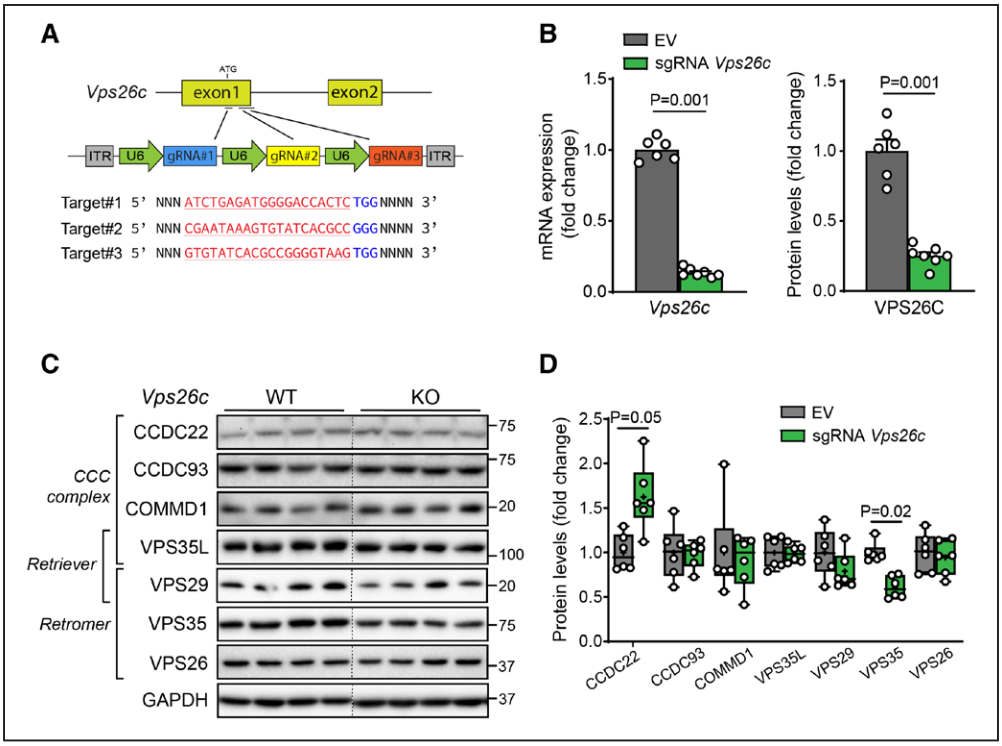

Figure 3. Hepatic VPS26C deficiency does not impair CCC complex stability.
A, Schematic illustration of single-vector AAV (adeno-associated virus) system used for targeting *Vps26c* in hepatic Cas9-expressing mice. Target sequences are shown in red and PAM sequences in blue. **B**, *Vps26c* mRNA and VPS26C protein expression (determined by targeted proteomics) in livers of mice, 4 weeks after CRISPR/Cas9-mediated targeting (n=6–7). Data are presented as mean±SEM; groups were compared using Welch *t* test. **C**, Hepatic protein levels of CCC complex, retriever, and retromer subunits determined by immunoblotting. Proteins in liver homogenates (n=6) were separated in the same gel and transferred to the same membrane for analysis; dotted line indicates different regions of the same gel. **D**, Quantification of immunoblot results shown in **C**. Data are presented as median with min-to-max whiskers (mean indicated by +); groups were compared using Mann-Whitney *U* test followed by multiple comparison correction.

these studies, the upregulation of LDLR was explained as a mechanism to compensate for the loss of LRP1 function.[8] Therefore, we speculated that the observed increase in LDLR protein levels could point to LRP1 dysfunction upon loss of VPS26C.

To investigate this in more depth, we used mouse hepatoma cells (Hepa1-6) to study the contribution of VPS26C to LDLR and LRP1 functioning. Using CRISPR/Cas9 technology, we ablated VPS26C (Figure 5A) and found that its loss had no marked effects on the protein expression of CCC subunits (Figure 5B; Figure S1B), while it slightly increased the subunits of retriever and retromer (Figure 5B; Figure S1C). VPS26C ablation significantly decreased the total levels, as well as the cell surface levels, of LRP1 (Figure 5C and 5D; Figure S1D), likely due to increased lysosomal degradation due to impaired endosomal recycling of LRP1,[24] whereas LDLR expression at the cell surface was increased without affecting total LDLR levels (Figure 5C and 5D). In addition, we performed GST-pulldown assays in HEK293T cells co-transfected with Flag-VPS26C and GST-tagged ICD of LDLR, or GST-tagged ICD of LRP1. Here, we observed a specific interaction between VPS26C and the ICD of LRP1, but not of LDLR (Figure 5E). Taken together, these findings suggest that VPS26C is required for the transport of LRP1—but not LDLR—from the endosome to the plasma membrane.

Hepatic VPS26C Is Required for LRP1-Mediated Uptake of Postprandial Triglyceride-Rich Lipoprotein Remnants

As mentioned previously, LDLR can compensate for the loss of LRP1 in the liver.[8] Thus, to examine the contribution of hepatic VPS26C to LRP1-mediated uptake of plasma lipids in mice, we blunted LDLR expression in their livers by using an AAV vector encoding the human gain-of-function variant PCSK9-D377Y.[49] This AAV was injected simultaneously with AAV expressing no sgRNAs or sgRNAs targeting *Vps26c* as used in the previous experiment (Figure 3A). Again, expressing the sgRNAs targeting *Vps26c* strongly downregulated VPS26C protein levels (Figure 6A), and hepatic expression of PCSK9-D377Y blunted hepatic LDLR expression (Figure 6B and 6C). In the absence of LDLR, loss of hepatic VPS26C did not affect plasma cholesterol levels (Figure 6D and 6E) or hepatic lipids (Figure S2A) but significantly increased plasma TG levels by 26% (Figure 6D). FPLC analysis showed that the increase in TGs was found mainly in the chylomicron remnants/VLDL and

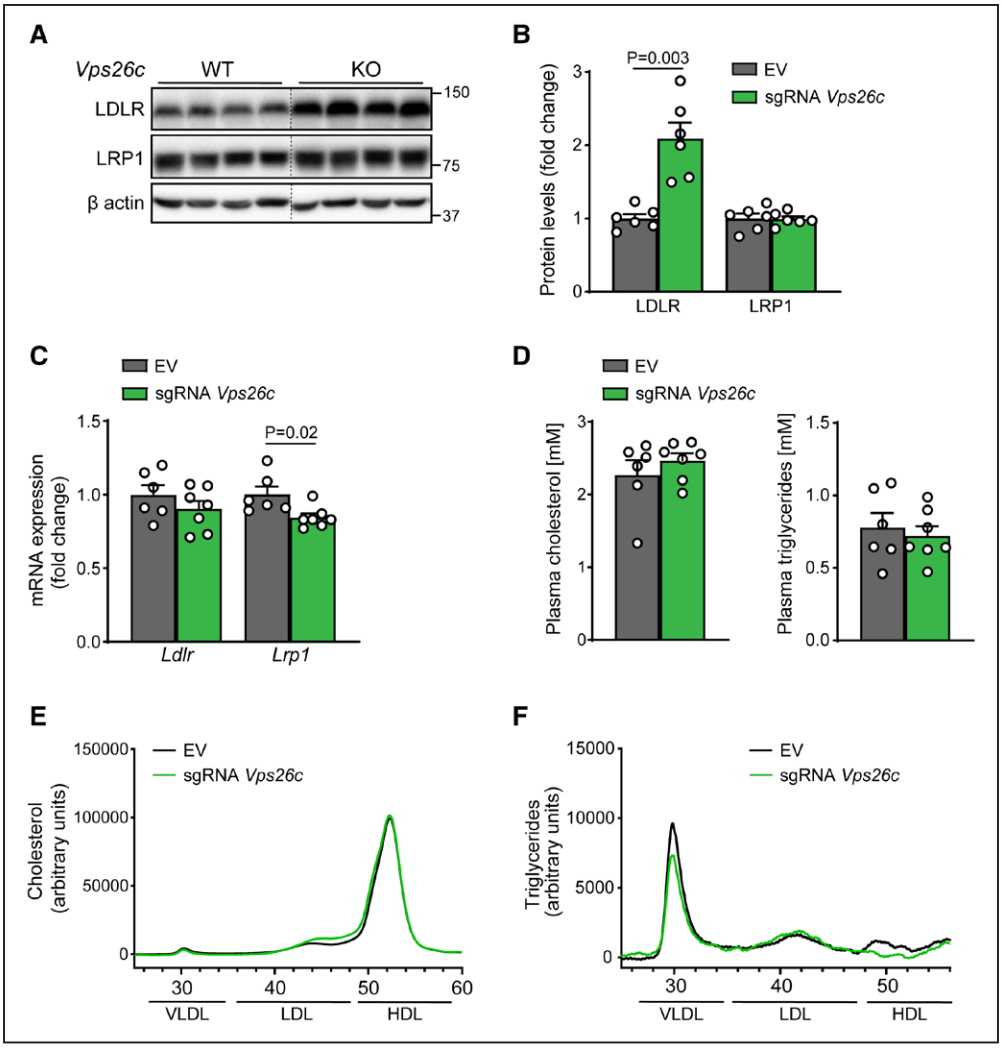

Figure 4. Loss of hepatic VPS26C increases low-density lipoprotein receptor (LDLR) protein levels but does not affect plasma lipids.

A, Immunoblot of LDLR and LRP1 (LDLR-related protein 1) in control and VPS26C-deficient livers. Proteins in liver homogenates (n=6) separated in the same gel and transferred to the same membrane for analysis; dotted line indicates different regions of the same gel. **B**, Quantification of immunoblot results shown in **A**. **C**, mRNA levels of *Ldlr* and *Lrp1* in control and VPS26C-deficient livers (n=6–7). **D**, Plasma cholesterol and triglyceride levels in control and hepatic VPS26C-deficient mice, 4 weeks after CRISPR/Cas9-mediated gene editing (n=5–7). **E**, Average cholesterol levels in plasma of control and hepatic VPS26C-deficient mice fractionated by FPLC (n=6 control mice and 7 hepatic VPS26C-deficient mice). **F**, Triglyceride levels in pooled plasma fractionated by FPLC of control and hepatic VPS26C-deficient mice (n=one pooled sample from 6 controls or 7 hepatic VPS26C-deficient mice), 4 weeks after CRISPR/Cas9-mediated gene editing. Data are presented as mean±SEM; groups are compared using Welch *t* test (**B**) and Student *t* test (**C** and **D**).

IDL (intermediate density lipoprotein)/LDL particle size range (Figure 6F). In addition, the apoB48/apoB100 ratio, a marker for remnant lipoproteins, in plasma of hepatic VPS26C-deficient mice with blunted LDLR levels was increased compared with control mice (Inset Figure 6F). An increase in apoB48/apoB100 ratio has also been observed in hepatic LRP1-deficient mice on a LDLR knockout background,[8] suggesting that VPS26C mediates LRP1 function. The increased TG levels were not caused by changes in VLDL secretion (Figure 6G), which led us to evaluate whether hepatic VPS26C deficiency impaired the clearance of postprandial TRL in the absence of LDLR. To this extent, we challenged the mice with an oral fat load and determined the clearance of TRL over time. We observed that TG clearance was significantly delayed in hepatic VPS26C-deficient mice compared with control mice (Figure 6H).

To determine whether this is solely a postprandial effect, we also assessed the hepatic uptake of VLDL-like particles.[42] After a glucose injection, mice were injected with VLDL-like particles, double-labeled with glycerol tri[^{3}H]oleate (TO) and [^{14}C]cholesteryl oleate (CO); we then determined the organ-specific uptake of the radiolabels. Under these conditions, hepatic VPS26C ablation in an LDLR-deficient background affected neither the hepatic uptake of [^{3}H]TO and [^{14}C]CO-derived activity, nor the plasma decay (Figure S2B and S2C). These results suggest that hepatic deletion of VPS26C

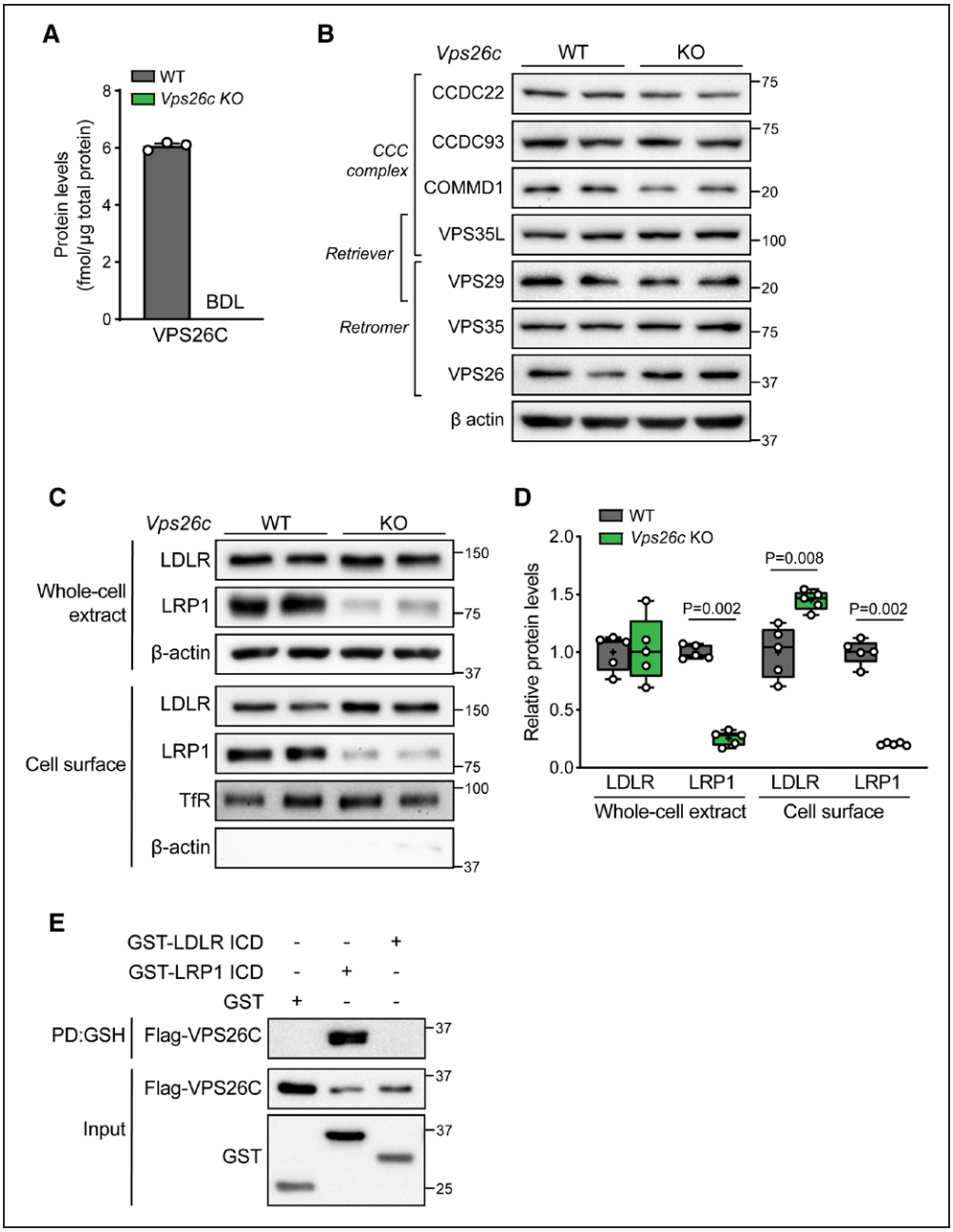

Figure 5. VPS26C is required for normal cell surface expression of LRP1 (low-density lipoprotein receptor [LDLR]-related protein 1).

A, VPS26C protein levels in wild-type (WT) and VPS26C-deficient (KO) Hepa1-6 cells, determined by targeted proteomics. **B**, Protein expression of CCC complex, retriever, and retromer subunits in Hepa1-6 WT and *Vps26c* knockout (KO) cells, determined by immunoblotting. **C**, Immunoblot of LDLR and LRP1 in whole-cell extracts and at the cell surface in control and VPS26C-deficient Hepa1-6 cells, determined by immunoblotting. Data represent 2 independent experiments. **D**, Quantification of total and cell surface LDLR and LRP1 protein levels in control and VPS26C-deficient Hepa1-6 cells of 2 independent experiments (n=5), as shown in **C**. **E**, Immunoblot of HEK293T cells transfected with Flag-VPS26C and either GST-LDLR intracellular domain (ICD), GST-LRP1 ICD, or GST alone, after performing a GST-pulldown assay to study the interaction between VPS26C and the ICD of LDLR or LRP1. Data represent 2 independent experiments. Data are presented as median with min-to-max whiskers (mean indicated by +; **D**); groups are compared using Mann-Whitney *U* test (**D**). BDL indicates below detection level.

specifically delays the uptake of postprandial TRL remnants, rather than VLDL-like particles, which may be explained by the different composition of these particles, such as the absence of apoB. Together, these findings indicate that hepatic VPS26C is needed for the hepatic clearance of postprandial TG-rich lipoproteins.

DISCUSSION

The retriever protein complex, consisting of VPS26C, VPS35L, and VPS29, was recently described as a novel endosomal sorting complex in the CCC-WASH axis to promote recycling of receptors back to the cell surface.[31]

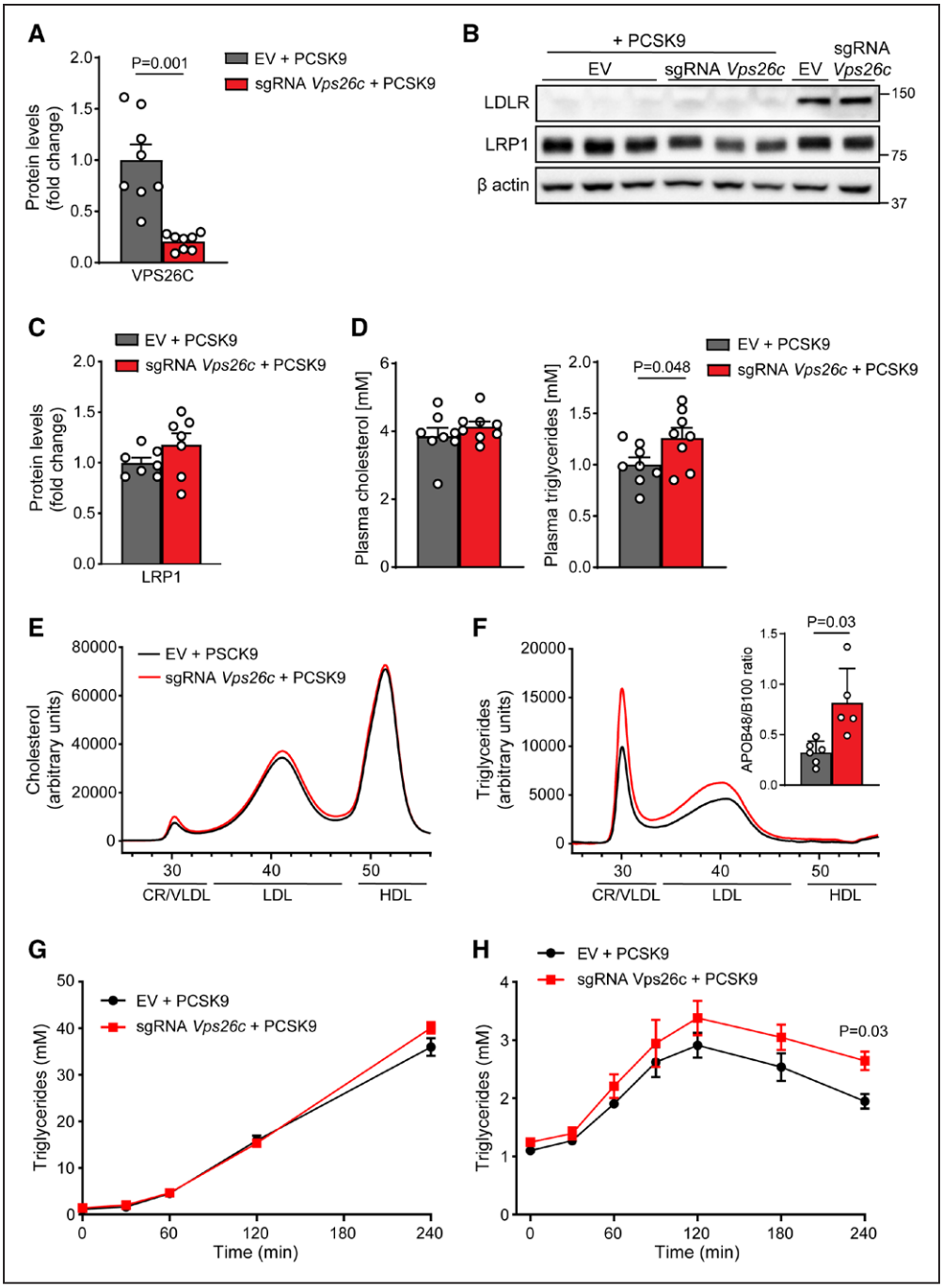

Figure 6. Hepatic VPS26C deficiency on a low-density lipoprotein receptor (LDLR)-deficient background increases plasma TG levels and decreases postprandial TG clearance.

A, VPS26C protein expression in livers of mice, 4 weeks after CRISPR/Cas9-mediated *Vps26c* targeting and AAV (adeno-associated virus)-PCSK9-D377Y administration (n=8), determined by targeted proteomics. **B**, Immunoblot of LDLR and LRP1 (LDLR-related protein 1) in control and VPS26C-deficient livers after AAV-PCSK9-D377Y administration. **C**, Quantification of total LRP1 protein levels in livers of control and hepatic VPS26C-deficient mice after AAV-PCSK9-D377Y administration (n=6–7), as determined by immunoblotting. **D**, Plasma cholesterol and triglyceride levels in control and hepatic VPS26C-deficient mice after AAV-PCSK9-D377Y administration (n=8). **E**, Average cholesterol in plasma of indicated groups (n=8) fractionated by FPLC. **F**, Average triglyceride levels in plasma of indicated groups fractionated by FPLC (n=7 control mice; 1 sample excluded due to technical issues and 6 hepatic VPS26C-deficient mice+AAV-PCSK9-D377Y; 2 samples excluded due to technical issues). (Inset **F**) Ratio of apoB48/apoB100 levels in plasma of indicated groups, as determined by targeted proteomics (n=5–6). **G**, Plasma triglyceride levels in indicated groups (n=7) following IP injection with poloxamer 407. **H**, Plasma triglyceride levels after olive oil bolus in 5-hour fasted control and hepatic VPS26C-deficient mice after AAV-PCSK9-D377Y administration (n=8–9). Data are presented as mean±SEM; groups are compared using Welch *t* test (**A**, inset **F**), Student *t* test (**C** and **D**) and repeated measures ANOVA with Geisser-Greenhouse correction and Šidák's multiple comparison test (**G** and **H**).

Here, we used somatic CRISPR/Cas9 gene-editing technology to systematically ablate VPS35L and VPS26C in mouse hepatocytes to elucidate their role in the endosomal recycling of LDLR and LRP1. We demonstrate that CCC complex formation does not completely rely on VPS35L but needs VPS35L for its function to transport LDLR and LRP1 from the endosome to the cell surface; thereby, VPS35L is also indispensable for maintaining plasma cholesterol homeostasis. On the other hand, our data show that retriever subunit VPS26C is required for hepatic uptake of postprandial TRL, by promoting surface expression of LRP1 but not LDLR, indicating that this retriever component has a cargo-selective role in CCC/WASH-mediated lipoprotein receptor transport.

Initially, VPS35L was recognized as forming the CCC complex, together with CCDC22, CCDC93, and the 10 COMMD proteins.[28] Although a later study described VPS35L as a component of retriever,[31] others proposed that VPS35L is a shared subunit between retriever and CCC,[37] or that both complexes represent one large multiprotein complex, COMMander.[39] Here, we found that loss of hepatic VPS35L reduces CCC core components CCDC93 and CCDC22 by only approximately 50% without a profound impact on COMMD proteins, but it strongly decreases VPS26C levels. In contrast, hepatic deficiency of CCDC22 or any COMMD protein reduces the protein levels of all CCC subunits, including VPS35L and VPS26C, by at least 70%[24,25] (Figure 1F). We also demonstrated that the composition of the CCC complex is minimally affected upon VPS35L ablation; only the association of CCDC22 with the CCC complex was reduced by 29%, while the other CCC core subunits were unaffected. Our data therefore favor the model that VPS35L is not a core subunit of the CCC complex, but is a shared component of CCC and retriever. However, VPS35L is apparently still essential for a functional CCC complex to inhibit WASH recruitment and activity,[37] as both VPS35L and CCC orchestrate the transport of LDLR and LRP1 to the cell surface, thereby controlling plasma cholesterol levels. This is in line with studies with HeLa cells, where selective ablation of either VPS35L, CCDC93, or COMMD3 has similar phenotypes, including impaired endosomal trafficking of GLUT1 (glucose transporter 1), due to increased recruitment and activity of the WASH complex on endosomes.[37]

Our data suggest that VPS35L is required for the physical association between the CCC complex and retriever, as VPS35L deficiency decreases VPS26C levels accompanied by abolished binding of the retriever subunit VPS29 to the CCC complex. In contrast, the total levels of VPS29 in mouse livers were not affected by the loss of VPS35L, but this can likely be explained by its presence in both retriever and retromer.[31] Consistent with this result, total protein levels of retromer subunits VPS35 and VPS26 were minimally or unaffected, suggesting that retromer is not disturbed by VPS35L deficiency. Since VPS29 is a subunit of retriever and retromer,[31] we did not inactivate VPS29 as it would negatively affect both complexes and would therefore complicate the interpretation of the results of this study. However, to fully understand the molecular organization of the endosomal sorting machinery and its role in lipid homeostasis, future studies are needed but this is beyond the scope of the current study.

Here, we also show that, similar to hepatic loss of VPS35L, deficiency of the CCC component COMMD1 strongly reduces the protein levels of retriever subunit VPS26C. Yet, functional assembly of the CCC complex in the CCC-WASH axis does not rely on VPS26C, as hepatic VPS26C deficiency neither affects CCC integrity, nor results in a hypercholesterolemic phenotype. Consistent with prior work,[31,37] our data suggest that VPS26C has a distinct function in the CCC-WASH axis to orchestrate endosomal cargo transport. Whereas CCC promotes surface expression of both LRP1 and LDLR,[24,25] VPS26C specifically facilitates the surface levels of LRP1, but not LDLR. This is evident from our results in cells deficient for VPS26C, where LRP1 levels are reduced both in the whole-cell lysate and at the plasma membrane and its binding to LRP1, but not LDLR. The decreased LRP1 surface levels can probably be explained by reduced endosomal receptor recycling, resulting in impaired retrieval of the receptor from lysosomal degradation.[24,25] Interestingly, the reduction of LRP1 levels is not observed in VPS26C-deficient total liver lysates. However, this observation is in line with our previous studies, where we observed that CCC deficiency reduces levels of both LDLR and LRP1 in the whole-cell lysate and plasma membrane of MEFs and primary hepatocytes, but not in total liver lysates.[24,25] The exact reason for this discrepancy is not known, but we speculate that it might be caused by the lack of cellular polarity when primary hepatocytes are grown in a monolayer.[50,51] Hepatocytes in vivo are polarized and contain an apical and basolateral surface with distinct sorting pathways[52]; losing the polarity might increase the lysosomal degradation of the receptors in CCC, WASH or retriever-deficient hepatocytes.

Impaired functioning of LRP1 upon hepatic VPS26C deficiency is supported by the increased protein expression of LDLR, likely due to a compensatory mechanism as reported in various previous mouse models with either a loss of LRP1 or impaired LRP1 trafficking.[8,9,11,48] In addition, in line with our results, this compensation did not lead to reduced plasma LDL cholesterol levels under chow-fed conditions.[8,9,11] However, in contrast to our cellular models, the total LRP1 levels are not reduced upon hepatic *Vps26c* ablation in mice, and because it is technically difficult to assess the surface levels of LRP1 in vivo, we can

therefore not rule out that the decreased TG clearance can be explained by other mechanisms. For example, it has been shown that hepatic LPL (lipoprotein lipase) plays also an important role in TG clearance.[53,54] Hepatic LPL deficiency increases plasma TG due to a decrease in postprandial TG clearance.[55] However, hepatic loss of LPL also results in elevated plasma cholesterol levels,[55] a phenotype which has not been observed in hepatic VPS26C-deficient mice. Moreover, hepatic ablation of the WASH subunit *Washc1* did not affect the plasma levels of hepatic LPL,[26] suggesting that the endosomal sorting system does not mediate hepatic LPL levels. Although additional research is needed, these data argue against a role of LPL in elevated plasma TG in hepatic VPS26C-deficient mice.

Interestingly, it has been postulated that endosomal recycling of LDLR and LRP1 is orchestrated by a direct interaction between VPS26C and the adaptor protein SNX17.[31] SNX17 regulates endosomal recycling by binding with its FERM-domain to NPxY motifs in intracellular domains of various proteins, including LDLR family members LDLR and LRP1.[32–36] However, as we found that VPS26C specifically interacts with the ICD of LRP1, but not with the ICD of LDLR, our data may implicate that VPS26C does not act together with SNX17 to facilitate endosomal recycling of both members of the LDLR family, but likely only of LRP1. It is currently unclear how VPS26C selectively mediates endosomal lipoprotein receptor transport, but it is important to note that slight differences exist between the NPxY motifs in the cytoplasmic tails of LDLR and LRP1. LRP1 contains a proximal NPTY motif, which is recognized by SNX17, as well as a distal NPVY motif; LDLR has only one NPVY motif, which can also be recognized by SNX17.[32,34–36] The distal NPxY motif of LRP1 is essential for postprandial TRL clearance.[56] Like hepatic VPS26C-deficient mice, mice carrying a mutation in the distal NPxY motif of LRP1 show hepatic upregulation of LDLR, and on an LDLR-deficient background these LRP1 mutant mice show elevated plasma TG levels due to delayed postprandial TRL clearance.[56] It has been demonstrated that LRP1 translocates in a postprandial state from the endosomes to the cell surface.[57] This translocation is likely mediated by insulin, as insulin can phosphorylate the tyrosine residue within the distal NPxY motif, resulting in dissociation of LRP1-adaptor protein PID1.[11] PID1 sequesters LRP1 in endosomes under fasting conditions. Loss of hepatic PID1 increases LDLR levels, and hepatic PID1 inactivation in LDLR knockout mice results in decreased postprandial TRL clearance, with subsequent plasma TG accumulation.[11] The results of these studies are comparable to those of the current study, where we show that VPS26C specifically orchestrates the surface expression of LRP1 for controlling plasma TG levels in a postprandial state.

The role of VPS26C in endosomal LRP1 transport under specific metabolic conditions is supported by the observation that the dyslipidemic phenotype of liver-specific VPS26C-deficient mice with blunted LDLR levels is rather mild compared with that of hepatic CCC knockout mice on an LDLR-deficient background. The latter model displays a marked increase in both plasma cholesterol and TG levels,[25] which is similar to the phenotype of hepatic LRP1-deficient mice on an LDLR knockout background,[8] suggesting that loss of CCC almost completely impairs hepatic LRP1 functioning. In contrast, hepatic VPS26C deficiency results only in an increase in plasma TG levels, with an effect size comparable to LDLR-deficient mice carrying a mutation in the distal NPxY motif of LRP1.[56] Based on these data we hypothesize that VPS26C recognizes specific members of the LDLR family within the retriever-CCC-WASH axis. Yet it remains to be determined how these cargos are recognized, whether VPS26C and PID1 are molecularly connected, whether VPS26C binds to the distal NPxY motif under specific conditions, and whether this interaction is SNX17-dependent, or if other adaptor proteins might be involved.

Additionally, it is important to note that mutations in the genes encoding retriever subunits are found in humans with developmental and neurological disorders. Recently, Kato et al[58] reported pathogenic variants in *VPS35L* in patients with a 3C/Ritscher-Schinzel (RSS)-like syndrome. Furthermore, a homozygous nonsense variant in *VPS26C* was described in individuals with a pleiotropic syndrome characterized by neurodevelopmental defects, growth failure, skeletal anomalies, and distinctive facial features.[59] Previous studies have already reported mutations in subunits of the CCC and WASH complexes that cause neurodevelopmental disorders. For example, mutations in *WASHC4* and *WASHC5* have been identified in patients with non-syndromic autosomal recessive intellectual disability[60] and 3C/RSS,[61] respectively, and mutations in *CCDC22* cause X-linked recessive intellectual disability (XLID) with clinical features of 3C/RSS.[62] We previously demonstrated that mutations in *CCDC22* and *WASHC5* cause hypercholesterolemia,[24–26] but whether mutations in *VPS35L* and *VPS26C* are also associated with increased plasma lipid levels remains to be evaluated. In addition, it is currently unclear whether metabolic stressors, including lipid accumulation, affect the functioning of the components of the endosomal sorting machinery. Using GENEVESTIGATOR[63] (Supplemental Material), we studied the mRNA levels of the subunits of retriever, retromer and the CCC complex in livers of non-alcoholic fatty liver disease (NAFLD)/non-alcoholic steatohepatitis (NASH) patients (Figure S3; Table S1). In several studies, only small changes for

some of the subunits were observed (Figure S3), but whether these changes have physiological consequences need to be determined. Furthermore, we cannot rule out that metabolic changes might influence these complexes at a post-translational level, which may affect their subcellular localization or association with their cargos. Future studies are therefore needed to better understand how metabolism and the endosomal system are intertwined.

Taken together, here, we report for the first time that retriever subunits VPS35L and VPS26C have specific functions in endosomal transport of lipoprotein receptors in hepatocytes. VPS35L participates in retriever and the CCC complex, while VPS26C is only a component of retriever. We show that VPS35L is needed for CCC functioning to orchestrate the endosomal transport of LDLR and LRP1 to control plasma cholesterol levels. VPS26C specifically facilitates the transport of LRP1, but not of LDLR, from the endosomes to the plasma membrane, and hereby controls postprandial TG levels in plasma. However, we cannot rule out other mechanisms explaining the increased plasma TG levels upon hepatic ablation of *Vps26c* in a LDLR-deficient background. Further studies are required to better understand the mechanism underlying cargo specificity; such understanding can augment our current knowledge of how receptor-mediated lipid uptake in the liver is tightly controlled.

ARTICLE INFORMATION

Received January 14, 2022; accepted October 26, 2022.

Affiliations

Department of Pediatrics, University of Groningen, University Medical Center Groningen, the Netherlands (D.Y.V., M.W., M.S., N.H., N.J.K., J.C.W., J.AK., B.v.d.S.). Institute for Diabetes and Cancer, Helmholtz Center Munich, Neuherberg, Germany. Joint Heidelberg-IDC Translational Diabetes Program, Inner Medicine 1, Heidelberg University Hospital, Germany (J.J.T.). German Center for Diabetes Research (DZD), Neuherberg, Germany (J.J.T.). Department of Medicine, Division of Endocrinology (A.C.M.P., S.K., P.C.N.R.) and Einthoven Laboratory for Experimental Vascular Medicine (A.C.M.P., S.K., P.C.N.R.), Leiden University Medical Center, the Netherlands.

Acknowledgments

The authors would like to acknowledge Ydwine van der Veen for technical assistance and Jörg Heeren for providing the construct containing the ICD of LRP1. In addition, we thank Philip Zimmermann for providing access to GENEVESTIGATOR and for his support with the data analysis.

Sources of Funding

This study was financially supported by grants from the European Union (Marie Skłodowska-Curie Actions Innovative Training Network (MSCA-ITN) 2020, 953489; Acronym EndoConnect) coordinated by B van de Sluis; The Netherlands Cardiovascular Research Initiative: "the Dutch Heart Foundation, Dutch Federation of University Medical Centers, The Netherlands Organization for Health Research and Development and the Royal Netherlands Academy of Sciences" (CVON2017-2020; Acronym Genius2) to P.C.N. Rensen, J. Albert Kuivenhoven and B. van de Sluis; the Groningen University Institute for Drug Exploration (GUIDE); and the De Cock-Hadders Foundation to D.Y. Vos, P.C.N. Rensen, and J. Albert Kuivenhoven are established investigators of the Netherlands Heart Foundation.

Disclosures

None.

Supplemental Material

Supplemental Methods
Figures S1–S4
Table S1
Major Resources Table
References[64,65]

REFERENCES

1. World Health Organization. Cardiovascular diseases (CVDs) [fact sheet]. https://www.who.int/en/news-room/fact-sheets/detail/cardiovascular-diseases-(cvds). Published 2021. Accessed October 6, 2021.
2. Ference BA, Ginsberg HN, Graham I, Ray KK, Packard CJ, Bruckert E, Hegele RA, Krauss RM, Raal FJ, Schunkert H, et al. Low-density lipoproteins cause atherosclerotic cardiovascular disease. 1. Evidence from genetic, epidemiologic, and clinical studies. A consensus statement from the European Atherosclerosis Society Consensus Panel. *Eur Heart J*. 2017;38:2459–2472. doi: 10.1093/eurheartj/ehx144
3. Nordestgaard BG, Varbo A. Triglycerides and cardiovascular disease. *Lancet*. 2014;384:626–635. doi: 10.1016/S0140-6736(14)61177-6
4. Ginsberg HN, Packard CJ, Chapman MJ, Borén J, Aguilar-Salinas CA, Averna M, Ference BA, Gaudet D, Hegele RA, Kersten S, et al. Triglyceride-rich lipoproteins and their remnants: metabolic insights, role in atherosclerotic cardiovascular disease, and emerging therapeutic strategies — a consensus statement from the European Atherosclerosis Society. *Eur Heart J*. 2021;42:4791–4806. doi: 10.1093/eurheartj/ehab551
5. Dieckmann M, Dietrich MF, Herz J. Lipoprotein receptors - an evolutionary ancient multifunctional receptor family. *Biol Chem*. 2010;391:1341–1363. doi: 10.1515/BC.2010.129
6. Goldstein JL, Brown MS, Anderson RGW, Russell DW, Schneider WJ. Receptor-mediated endocytosis: concepts emerging from the LDL receptor system. *Ann Rev Cell Biol*. 1985;1:1–39. doi: 10.1146/annurev.cb.01.110185.000245
7. Ishibashi S, Herz J, Maedat N, Goldstein JL, Brown MS. The two-receptor model of lipoprotein clearance: tests of the hypothesis in "knockout" mice lacking the low density lipoprotein receptor, apolipoprotein E, or both proteins. *Proc Natl Acad Sci*. 1994;91:4431–4435.
8. Rohlmann A, Gotthardt M, Hammer RE, Herz J. Inducible inactivation of hepatic LRP gene by cre-mediated recombination confirms role of lrp in clearance of chylomicron remnants. *J Clin Invest*. 1998;101:689–695. doi: 10.1172/JCI1240
9. Gordts PL, Bartelt A, Nilsson SK, Annaert W, Christoffersen C, Nielsen LB, Heeren J, Roebroek AJ. Impaired LDL receptor-related protein 1 translocation correlates with improved dyslipidemia and atherosclerosis in apoE-deficient mice. *PLoS One*. 2012;7:1–12. doi: 10.1371/journal.pone.0038330
10. Foley EM, Gordts PLSM, Stanford KI, Gonzales JC, Stoddard N, Esko JD. Hepatic remnant lipoprotein clearance by heparan sulfate proteoglycans and low-density lipoprotein receptors depend on dietary conditions in mice. *Arterioscler Thromb Vasc Biol*. 2013;33:2065–2074. doi: 10.1161/ATVBAHA.113.301637.Hepatic
11. Fischer AW, Albers K, Krott LM, Hoffzimmer B, Heine M, Schmale H, Scheja L, Gordts PLSM, Heeren J. The adaptor protein PID1 regulates receptor-dependent endocytosis of postprandial triglyceride-rich lipoproteins. *Mol Metab*. 2018;16:88–99. doi: 10.1016/j.molmet.2018.07.010
12. Teslovich TM, Musunuru K, Smith AV, Edmondson AC, Stylianou IM, Koseki M, Pirruccello JP, Ripatti S, Chasman DI, Willer CJ, et al. Biological, clinical and population relevance of 95 loci for blood lipids. *Nature*. 2010;466:707–713. doi: 10.1038/nature09270
13. Willer CJ, Schmidt EM, Sengupta S, Peloso GM, Gustafsson S, Kanoni S, Ganna A, Chen J, Buchkovich ML, Mora S, et al; Global Lipids Genetics Consortium. Discovery and refinement of loci associated with lipid levels. *Nat Genet*. 2013;45:1274–1283. doi: 10.1038/ng.2797
14. Goldstein JL, DeBose-Boyd RA, Brown MS. Protein sensors for membrane sterols. *Cell*. 2006;124:35–46. doi: 10.1016/j.cell.2005.12.022
15. Lagace TA, Curtis DE, Garuti R, McNutt MC, Park SW, Prather HB, Anderson NN, Ho YK, Hammer RE, Horton JD. Secreted PCSK9 decreases the number of LDL receptors in hepatocytes and in livers of parabiotic mice. *J Clin Invest*. 2006;116:2995–3005. doi: 10.1172/JCI29383
16. Zhang D-W, Lagace TA, Garuti R, Zhao Z, McDonald M, Horton JD, Cohen JC, Hobbs HH. Binding of proprotein convertase Subtilisin/ Kexin Type 9 to epidermal growth factor-like repeat a of low density lipoprotein receptor decreases receptor recycling and increases degradation. *J Biol Chem*. 2007;282:18602–18612. doi: 10.1074/jbc.M702027200

17. Poirier S, Mayer G, Poupon V, McPherson PS, Desjardins R, Ly K, Asselin M-C, Day R, Duclos FJ, Witmer M, et al. Dissection of the endogenous cellular pathways of PCSK9-induced low density lipoprotein receptor degradation. *J Biol Chem*. 2009;284:28856–28864. doi: 10.1074/jbc.M109.037085
18. Zelcer N, Hong C, Boyadjian R, Tontonoz P. LXR Regulates cholesterol uptake through idol-dependent ubiquitination of the LDL receptor. *Science*. 2009;325:100–104. doi: 10.1126/science.1168974
19. Scotti E, Calamai M, Goulbourne CN, Zhang L, Hong C, Lin RR, Choi J, Pilch PF, Fong LG, Zou P, et al. IDOL stimulates clathrin-independent endocytosis and multivesicular body-mediated lysosomal degradation of the low-density lipoprotein receptor. *Mol Cell Biol*. 2013;33:1503–1514. doi: 10.1128/MCB.01716-12
20. Wijers M, Kuivenhoven JA, Van De Sluis B. The life cycle of the low-density lipoprotein receptor: Insights from cellular and in-vivo studies. *Curr Opin Lipidol*. 2015;26:82–87. doi: 10.1097/MOL.0000000000000157
21. Van De Sluis B, Wijers M, Herz J. News on the molecular regulation and function of hepatic LDLR and LRP1. *Curr Opin Lipidol*. 2017;28:241–247. doi: 10.1097/MOL.0000000000000411
22. Vos DY, Van De Sluis B. Function of the endolysosomal network in cholesterol homeostasis and metabolic- associated fatty liver disease (MAFLD). *Mol Metab*. 2021;50:101146. doi: 10.1016/j.molmet.2020.101146
23. Goldstein JL, Brown MS, Anderson RGW. Coated pits, coated vesicles, and receptor-mediated endocytosis. *Nature*. 1979;279:679–685. doi: 10.1038/279679a0
24. Bartuzi P, Billadeau DD, Favier R, Rong S, Dekker D, Fedoseienko A, Fieten H, Wijers M, Levels JH, Huijkman N, et al. CCC- and WASH-mediated endosomal sorting of LDLR is required for normal clearance of circulating LDL. *Nat Commun*. 2016;7:1–11. doi: 10.1038/ncomms10961
25. Fedoseienko A, Wijers M, Wolters JC, Dekker D, Smit M, Huijkman N, Kloosterhuis N, Klug H, Schepers A, Willems van Dijk K, et al. COMMD family regulates plasma LDL levels and attenuates atherosclerosis through stabilizing the CCC complex in endosomal LDLR trafficking. *Circ Res*. 2018;122:1648–1660. doi: 10.1161/CIRCRESAHA.117.312004
26. Wijers M, Zanoni P, Liv N, Vos DY, Jäckstein MY, Smit M, Wilbrink S, Wolters JC, van der Veen YT, Huijkman N, et al. The hepatic WASH complex is required for efficient plasma LDL and HDL cholesterol clearance. *JCI Insight*. 2019;4:e126462. doi: 10.1172/jci.insight.126462
27. Rimbert A, Dalila N, Wolters JC, Huijkman N, Smit M, Kloosterhuis N, Riemsma M, van der Veen Y, Singla A, van Dijk F, et al; Biobank-Based Integrative Omics Studies Consortium. A common variant in CCDC93 protects against myocardial infarction and cardiovascular mortality by regulating endosomal trafficking of low-density lipoprotein receptor. *Eur Heart J*. 2020;41:1040–1053. doi: 10.1093/eurheartj/ehz727
28. Phillips-Krawczak CA, Singla A, Starokadomskyy P, Deng Z, Osborne DG, Li H, Dick CJ, Gomez TS, Koenecke M, Zhang J-S, et al. COMMD1 is linked to the WASH complex and regulates endosomal trafficking of the copper transporter ATP7A. *Mol Biol Cell*. 2015;26:91–103. doi: 10.1091/mbc.E14-06-1073
29. Harbour ME, Breusegem SY, Seaman MNJ. Recruitment of the endosomal WASH complex is mediated by the extended "tail" of Fam21 binding to the retromer protein Vps35. *Biochem J*. 2012;442:209–220. doi: 10.1042/BJ20111761
30. Wang J, Fedoseienko A, Chen B, Burstein E, Jia D, Billadeau DD. Endosomal receptor trafficking: retromer and beyond. *Traffic*. 2018;578:590. doi: 10.1111/tra.12574
31. McNally KE, Faulkner R, Steinberg F, Gallon M, Ghai R, Pim D, Langton P, Pearson N, Danson CM, Nägele H, et al. Retriever is a multiprotein complex for retromer-independent endosomal cargo recycling. *Nat Cell Biol*. 2017;19:1214–1225. doi: 10.1038/ncb3610
32. Burden JJ, Sun X-M, García García AB, Soutar AK. Sorting motifs in the intracellular domain of the low density lipoprotein receptor interact with a novel domain of sorting Nexin-17. *J Biol Chem*. 2004;279:16237–16245. doi: 10.1074/jbc.M313689200
33. Stockinger W, Sailler B, Strasser V, Recheis B, Fasching D, Kahr L, Schneider WJ, Nimpf J. The PX-domain protein SNX17 interacts with members of the LDL receptor family and modulates endocytosis of the LDL receptor. *EMBO J*. 2002;21:4259–4267. doi: 10.1093/emboj/cdf435
34. Van Kerkhof P, Lee J, McCormick L, Tetrault E, Lu W, Schoenfish M, Oorschot V, Strous GJ, Klumperman J, Bu G. Sorting nexin 17 facilitates LRP recycling in the early endosome. *EMBO J*. 2005;24:2851–2861. doi: 10.1038/sj.emboj.7600756
35. Farfan P, Lee J, Larios J, Sotelo P, Bu G, Marzolo M-P. A Sorting Nexin 17-binding domain within the lrp1 cytoplasmic tail mediates receptor recycling through the basolateral sorting endosome. *Traffic*. 2013;14:823–838. doi: 10.1111/tra.12076
36. Donoso M, Cancino J, Lee J, van Kerkhof P, Retamal C, Bu G, Gonzalez A, Cáceres A, Marzolo M-P. Polarized traffic of LRP1 Involves AP1B and SNX17 operating on y-dependent sorting motifs in different pathways. *Mol Biol Cell*. 2009;20:481–497. doi: 10.1091/mbc.e08-08-0805
37. Singla A, Fedoseienko A, Giridharan SSP, Overlee BL, Lopez A, Jia D, Song J, Huff-Hardy K, Weisman L, Burstein E, et al. Endosomal PI(3)P regulation by the COMMD/CCDC22/CCDC93 (CCC) complex controls membrane protein recycling. *Nat Commun*. 2019;10:4271. doi: 10.1038/s41467-019-12221-6
38. Burstein E, Hoberg JE, Wilkinson AS, Rumble JM, Csomos RA, Komarck CM, Maine GN, Wilkinson JC, Mayo MW, Duckett CS. COMMD proteins, a novel family of structural and functional homologs of MURR1. *J Biol Chem*. 2005;280:22222–22232. doi: 10.1074/jbc.M501928200
39. Mallam AL, Marcotte EM. Systems-wide studies uncover Commander, a multiprotein complex essential to human development. *Cell Syst*. 2017;4:483–494. doi: 10.1016/j.cels.2017.04.006
40. Platt RJ, Chen S, Zhou Y, Yim MJ, Swiech L, Kempton HR, Dahlman JE, Parnas O, Eisenhaure TM, Jovanovic M, et al. CRISPR-Cas9 knockin mice for genome editing and cancer modeling. *Cell*. 2014;159:440–455. doi: 10.1016/j.cell.2014.09.014
41. Vonk WIM, Bartuzi P, de Bie P, Kloosterhuis N, Wichers CGK, Berger R, Haywood S, Klomp LWJ, Wijmenga C, van de Sluis B. Liver-specific Commd1 knockout mice are susceptible to hepatic copper accumulation. *PLoS One*. 2011;6:e29183. doi: 10.1371/journal.pone.0029183
42. Rensen PCN, Herijgers N, Netscher MH, Meskers SCJ, van Eck M, van Berkel TJC. Particle size determines the specificity of emulsions for the LDL receptor versus hepatic remnant receptor in vivo. *J Lipid Res*. 1997;38:1070–1084. doi: 10.1016/s0022-2275(20)37190-x
43. Bligh EG, Dyer WJ. A rapid method of total lipid extraction and purification. *Can J Biochem Physiol*. 1959;37:911–917. doi:10.1139/o59-099
44. Daugherty A, Tall AR, Daemen MJ, Falk E, Fisher EA, García-Cardeña G, Lusis AJ, Owens iii AP, Rosenfeld ME, Virmani R. Recommendation on design, execution, and reporting of animal atherosclerosis studies: a scientific statement from the American Heart Association. *Arter Thromb Vasc Biol*. 2017;37:e131–e157. doi: 10.1161/ATV.0000000000000062
45. Nathwani AC, Gray JT, Ng CY, Zhou J, Spence Y, Waddington SN, Tuddenham EGD, Kemball-Cook G, McIntosh J, Boon-Spijker M, et al. Self-complementary adeno-associated virus vectors containing a novel liver-specific human factor IX expression cassette enable highly efficient transduction of murine and nonhuman primate liver. *Blood*. 2006;107:2653–2661. doi: 10.1182/blood-2005-10-4035
46. Zolotukhin S, Byrne BJ, Mason E, Zolotukhin I, Potter M, Chesnut K, Summerford C, Samulski RJ, Muzyczka N. Recombinant adeno-associated virus purification using novel methods improves infectious titer and yield. *Gene Ther*. 1999;6:973–985. doi: 10.1038/sj.gt.3300938
47. Loregger A, Raaben M, Nieuwenhuis J, Tan JME, Jae LT, van den Hengel LG, Hendrix S, van den Berg M, Scheij S, Song J-Y, et al. Haploid genetic screens identify SPRING/C12ORF49 as a determinant of SREBP signaling and cholesterol metabolism. *Nat Commun*. 2020;11:1128. doi: 10.1038/s41467-020-14811-1
48. Jaeschke A, Haller A, Cash JG, Nam C, Igel E, Roebroek AJM, Hui DY. Mutation in the distal NPxY motif of LRP1 alleviates dietary cholesterol-induced dyslipidemia and tissue inflammation. *J Lipid Res*. 2021;62:100012. doi: 10.1194/jlr.RA120001141
49. Bjørklund MM, Hollensen AK, Hagensen MK, Dagnaes-Hansen F, Christoffersen C, Mikkelsen JG, Bentzon JF. Induction of atherosclerosis in mice and hamsters without germline genetic engineering. *Circ Res*. 2014;114:1684–1689. doi: 10.1161/CIRCRESAHA.114.302937
50. van Beest M, Robben JH, Savelkoul PJM, Hendriks G, Devonald MA, Konings IB, Lagendijk AK, Karet F, Deen PM. Polarisation, key to good localisation. *Biochim Biophys Acta Biomembr*. 2006;1758:1126–1133. doi: 10.1016/j.bbamem.2006.03.007
51. Zeigerer A, Wuttke A, Marsico G, Seifert S, Kalaidzidis Y, Zerial M. Functional properties of hepatocytes in vitro are correlated with cell polarity maintenance. *Exp Cell Res*. 2017;350:242–252. doi: 10.1016/j.yexcr.2016.11.027
52. Apodaca G, Gallo LI, Bryant DM. Role of membrane traffic in the generation of epithelial cell asymmetry. *Nat Cell Biol*. 2012;14:1235–1243. doi: 10.1038/ncb2635
53. Merkel M, Weinstock PH, Chajek-Shaul T, Radner H, Yin B, Breslow JL, Goldberg IJ. Lipoprotein lipase expression exclusively in liver. A mouse model for metabolism in the neonatal period and during cachexia. *J Clin Invest*. 1998;102:893–901. doi: 10.1172/JCI2912

54. Merkel M, Eckel RH, Goldberg IJ. Lipoprotein lipase: genetics, lipid uptake, and regulation. *J Lipid Res*. 2002;43:1997–2006. doi: 10.1194/jlr.r200015-jlr200
55. Liu G, Xu JN, Liu D, Ding Q, Liu M-N, Chen R, Fan M, Zhang Y, Zheng C, Zou D-J, et al. Regulation of plasma lipid homeostasis by hepatic lipoprotein lipase in adult mice. *J Lipid Res*. 2016;57:1155–1161. doi: 10.1194/jlr.M065011
56. Gordts PLSM, Reekmans S, Lauwers A, Dongen AV, Verbeek L, Roebroek AJM. Inactivation of the LRP1 intracellular NPxYxxL Motif in LDLR-deficient mice enhances postprandial dyslipidemia and atherosclerosis. *Arterioscler Thromb Vasc Biol*. 2009;29:1258–1264. doi: 10.1161/ATVBAHA.109.192211
57. Laatsch A, Merkel M, Talmud PJ, Grewal T, Beisiegel U, Heeren J. Insulin stimulates hepatic low density lipoprotein receptor-related protein 1 (LRP1) to increase postprandial lipoprotein clearance. *Atherosclerosis*. 2009;204:105–111. doi: 10.1016/j.atherosclerosis.2008.07.046
58. Kato K, Oka Y, Muramatsu H, Vasilev FF, Otomo T, Oishi H, Kawano Y, Kidokoro H, Nakazawa Y, Ogi T, et al. Biallelic VPS35L pathogenic variants cause 3C/Ritscher-Schinzel-like syndrome through dysfunction of retriever complex. *J Med Genet*. 2020;57:245–253. doi: 10.1136/jmedgenet-2019-106213
59. Beetz C, Bauer P, Kdissa A, Sutton VR, Karageorgou V, Suleiman J. VPS26C homozygous nonsense variant in two cousins with neurodevelopmental deficits, growth failure, skeletal abnormalities, and distinctive facial features. *Clin Genet*. 2020;97:644–648. doi: 10.1111/cge.13690
60. Ropers F, Derivery E, Hu H, Garshasbi M, Karbasiyan M, Herold M, Nürnberg G, Ullmann R, Gautreau A, Sperling K, et al. Identification of a novel candidate gene for non-syndromic autosomal recessive intellectual disability: the WASH complex member swip. *Hum Mol Genet*. 2011;20:2585–2590. doi: 10.1093/hmg/ddr158
61. Elliott AM, Simard LR, Coghlan G, Chudley AE, Chodirker BN, Greenberg CR, Burch T, Ly V, Hatch GM, Zelinski T. A novel mutation in KIAA0196: Identification of a gene involved in Ritscher-Schinzel/3C syndrome in a first nations cohort. *J Med Genet*. 2013;50:819–822. doi: 10.1136/jmedgenet-2013-101715
62. Kolanczyk M, Krawitz P, Hecht J, Hupalowska A, Miaczynska M, Marschner K, Schlack C, Emmerich D, Kobus K, Kornak U, et al. Missense variant in CCDC22 causes X-linked recessive intellectual disability with features of Ritscher-Schinzel/3C syndrome. *Eur J Hum Genet*. 2015;23:633–638. doi: 10.1038/ejhg.2014.109
63. Hruz T, Laule O, Szabo G, et al. Genevestigator V3: A Reference Expression Database for the Meta-Analysis of Transcriptomes. *Adv Bioinformatics*. 2008;2008:1–5. doi: 10.1155/2008/420747
64. RStudio Team. RStudio: Integrated Development for R. RStudio, PBC, Boston, MA; 2020. http://www.rstudio.com/
65. Wickham H. ggplot2: Elegant Graphics for Data Analysis. Springer-Verlag New York; 2016. https://ggplot2.tidyverse.org